Blood, lead and spheres

A hindered settling equation for sedimentologists based on metadata analysis

Baas, Jaco H.; Baker, Megan L.; Buffon, Patricia; Strachan, Lorna J.; Bostock, Helen C; Hodgson, David; Eggenhuisen, Joris T.; Spychala, Yvonne T.

DOI
10.1002/dep2.176

Publication date
2022

Document Version
Final published version

Published in
Depositional Record

Received: 1 October 2021 | Revised: 24 January 2022 | Accepted: 25 January 2022

DOI: 10.1002/dep2.176

The Depositional Record
A journal of the International Association of Sedimentologists
Open Access
IAS
WILEY

ORIGINAL ARTICLE

Blood, lead and spheres: A hindered settling equation for sedimentologists based on metadata analysis

Jaco H. Baas[1] | **Megan L. Baker**[2] | **Patricia Buffon**[3] | **Lorna J. Strachan**[4] | **Helen C. Bostock**[5] | **David Hodgson**[6] | **Joris T. Eggenhuisen**[7] | **Yvonne T. Spychala**[8]

[1]School of Ocean Sciences, Bangor University, Wales, UK

[2]Department of Geography, Durham University, Durham, UK

[3]Department of Hydraulic Engineering, Delft University of Technology, Delft, the Netherlands

[4]School of Environment, University of Auckland, Aotearoa, New Zealand

[5]School of Earth and Environmental Science, University of Queensland, Brisbane, Australia

[6]School of Earth & Environment, University of Leeds, West Yorkshire, UK

[7]Faculty of Geosciences, Utrecht University, Utrecht, the Netherlands

[8]Institute of Geology, Leibniz Universität, Hannover, Germany

Correspondence
Jaco H. Baas, School of Ocean Sciences, Bangor University, Wales, UK.
Email: j.baas@bangor.ac.uk

Abstract

A revision of the popular equation of Richardson and Zaki (1954a, Transactions of the Institute of Chemical Engineering, 32, 35–53) for the hindered settling of suspensions of non-cohesive particles in fluids is proposed, based on 548 data sets from a broad range of scientific disciplines. The new hindered settling equation enables predictions of settling velocity for a wide range of particle sizes and densities, and liquid densities and viscosities, but with a focus on sediment particles in water. The analysis of the relationship between hindered settling velocity and particle size presented here shows that the hindered settling effect increases as the particle size decreases, for example, a 50% reduction in settling velocity is reached for 0.025 mm silt and 4 mm pebbles at particle concentrations of 13% and 25% respectively. Moreover, hindered settling starts to influence the settling behaviour of sediment particles at volumetric concentrations of merely a few per cent. For example, the particle settling velocity in flows that carry 5% silt is reduced by at least 22%. These observations suggest that hindered settling greatly increases the efficiency of natural flows to transport sediment particles, but also particulate carbon and pollutants, such as plastics, over large distances.

KEYWORDS

hindered settling, metadata analysis, particle fall velocity

1 | INTRODUCTION

The terminal fall velocity or settling velocity of solid particles in a fluid is a pivotal physical parameter in sedimentology (Dietrich, 1982). It lies at the heart of controlling the properties of sedimentary deposits, including their three-dimensional shape and size, and their internal texture and structure (Pyles et al., 2013). Moreover, the settling velocity governs the ease with which particles can be transported in suspension or as bedload by, for example, rivers and density currents. Because the settling velocity depends in part on the submerged weight of a particle, it also works against kinematic processes that try to lift particles from the bed in rivers, lakes, seas and oceans. Since the formulation of Stokes' law for the settling velocity of particles with small Reynolds numbers in a viscous fluid (Stokes, 1851), the settling velocity has been used universally, either explicitly or implicitly, in sedimentological research. This includes numerical modelling of sediment transport rates in modern environments and as a proxy for flow energy, rate of deposition and deposit runout distance stored in sedimentary rocks (Bell et al., 2021; Spychala et al., 2020). These applications go beyond Stokes' law, based on extensive research devoted to the settling velocity parameterisations that are valid outside the Stokes' range, for which particle Reynolds numbers are larger than one (Dietrich, 1982; van Rijn, 1993; Soulsby, 1997; Wu & Wang, 2006).

The settling velocity of individual non-cohesive particles depends on the particle diameter, the particle density, the liquid density and the viscosity of the fluid. However, it is widely known that the settling velocity also depends on the particle shape and shape distribution (Baldock et al., 2004; Beňa et al., 1963; Camenen, 2007; Chianese et al., 1992; Chong et al., 1979; Cleasby & Fan, 1981; Di Felice, 1995; Dietrich, 1982; Ferguson & Church, 2004; Fouda & Capes, 1977; Komar & Reimers, 1978; Maude & Whitmore, 1958; Richardson & Zaki, 1954a; Steinour, 1944b), the presence of adjacent particles (Carey, 1987; Pal & Ghoshal, 2013; Richardson & Zaki, 1954a, 1954b) and the particle size distribution (Di Felice, 1995; Hoffman et al., 1960; Lockett & Al-Habbooby, 1974; Maude & Whitmore, 1958; Mirza & Richardson, 1979; Richardson & Meikle, 1961; Scott & Mandersloot, 1979; Wilson, 1953).

The presence of adjacent particles in a suspension causes the hindered settling effect, in which flow around the neighbouring falling particles causes a larger fluid drag than for a single falling particle, resulting in a reduction of the fall velocity of individual particles in the suspension (Richardson & Zaki, 1954a, 1954b). The hindered settling effect has a strong influence on the settling behaviour of particles in dense suspensions, reducing the settling velocity by up to several orders of magnitude (Richardson & Zaki, 1954a, 1954b), and therefore significantly modifying the kinematic behaviour of sediment in transport and the properties of sedimentary deposits. In aqueous environments, the hindered settling effect is particularly important in hyperconcentrated river flows, high-density turbidity currents, subaqueous debris flows and other suspensions from which sediment particles settle out at high concentration. However, hindered settling is not confined to sedimentological applications. Dense suspensions of settling particles are also relevant to applications in, for example, medical science, food science and hydraulic and chemical engineering (Supplementary Table S1). This has resulted in a broad range of hindered settling studies, covering different particles, from sand and glass spheres to blood cells and tapioca, and different liquids, from water and oil to glycerol and alcohol. These studies have mostly focussed on single fields of research, matching the field of expertise of the authors. Hence, equations for fall velocity under hindered settling conditions are typically confined to several tens of data points.

The aim of this paper is to develop a new empirical equation for hindered settling of non-cohesive particles that expands the commonly used equation of Richardson and Zaki (1954a) by integrating 53 studies and 548 data sets from a wide range of disciplines. This metadata approach assumes that the particle fall velocity is independent of the type of particle and type of liquid, as it can be scaled based on basic particle and liquid properties, so the new equation can be used with more confidence than existing equations in sedimentology and other disciplines. This paper also provides evidence that the hindered settling effect starts to influence the fall velocity of particles at volumetric concentrations of only several per cent, especially for quartz silt and very fine sand in water. Application of the simple hindered settling equation presented in this paper should therefore be considered in a broad range of sedimentological studies.

2 | HINDERED SETTLING

2.1 | Principal measurement methods

Since early efforts in quantifying the settling rate of particle suspensions (Kermack et al., 1930; Robinson, 1926), hindered settling has been studied in the laboratory by means of two main methods (Barnea & Mizrahi, 1973): the settling column method (Wilson, 1953) and the fluidisation method (Wilhelm & Kwauk, 1948). In the settling column method, a well-mixed particulate suspension is allowed to settle in a tall container and the bulk settling velocity is determined from the distance settled of a lutocline at the top of the suspension per unit time. In the fluidisation method, a deposit is fluidised by forcing a fluid through the base of the deposit at constant discharge. The thickness of the fluidised suspension provides the equilibrium concentration of the particulate suspension at the applied discharge. This, in turn, is converted to the bulk settling velocity of the suspension by dividing the discharge by the cross-sectional area of the container. The settling column and fluidisation methods have been used interchangeably and shown to yield similar, method-independent, hindered settling velocities (Barnea & Mizrahi, 1973; Happel & Epstein, 1954; Loeffler, 1953; Loeffler & Ruth, 1959; Richardson & Meikle, 1961; Richardson & Zaki, 1954a).

2.2 | Hindered settling parameterisations

Many formulations for the hindered settling effect have been proposed since the first half of the 20th century (reviewed by Barnea & Mizhari, 1973; Di Felice, 1995;

Garside & Al-Dibouni, 1977; Khan & Richardson, 1989; Scott, 1984). Most of these formulations are at least partly based on empirical relationships between particle properties, liquid properties, suspended sediment concentration and single-particle settling velocity (Beňa et al., 1963; Garside & Al-Dibouni, 1977; Godard & Richardson, 1969; Jottrand, 1952; Khan & Richardson, 1989; Kynch, 1959; Lewis & Bowerman, 1952; Lewis et al., 1949; Ramamurthy & Subbaraju, 1973; Richardson & Zaki, 1954a; Rowe, 1987; Shannon et al., 1963; Watanabe, 1978; Wen & Fan, 1974; Wen & Yu, 1966). Other formulations have been based primarily on physical theory, often using computational fluid dynamics, or modifications of Stokes' law and Darcy's law (Brauer & Kriegel, 1966; Brinkman, 1949; Cheng, 1997; Di Felice, 1996; Foscolo et al., 1983; Happel, 1958; Letan, 1974; Loeffler & Ruth, 1959; Oliver, 1961; Richardson & Zaki, 1954b; Robinson, 1926; Steinour, 1944a; te Slaa et al., 2015; Zuber, 1964). However, the empirical equation of Richardson and Zaki (1954a) is still the most widely applied equation, because of its simplicity and perceived accuracy, as summarised by Di Felice (1995): '... supposed improvements of the original Richardson-Zaki equation have been suggested. In general, the predictive capability does not change significantly in spite of increased complexity and the use of non-justifiable factors'.

The Richardson and Zaki (1954a) equation relates the hindered settling velocity, $w_{s,h}$, to the settling velocity of a single particle, $w_{s,0}$, and the volumetric suspended particle concentration, C, through a coefficient m:

$$w_{s,h} = w_{s,0}\,(1-C)^{m} \tag{1}$$

where m depends on the particle diameter, D, via the particle Reynolds number, Re_p:

$$Re_p = \frac{w_{s,0}D}{\nu} \tag{2}$$

where ν is the kinematic viscosity of the fluid. Based on 60 series of settling velocity experiments with different particle densities and shapes, and different fluid densities and viscosities, Richardson and Zaki (1954a) proposed the following relationships between Re_p and m:

$$\begin{aligned} m &= 4.65 \text{ for } Re_p \le 0.2 \text{ (viscous regime)} \\ m &= 4.35\, Re_p^{-0.03} \text{ for } 0.2 < Re_p \le 1 \text{ (transitional regime)} \\ m &= 4.45\, Re_p^{-0.1} \text{ for } 1 < Re_p < 500 \text{ (transitional regime)} \\ m &= 2.39 \text{ for } Re_p \ge 500 \text{ (inertial regime)} \end{aligned} \tag{3}$$

Rowe (1987) expressed this dependency of m on Re_p in a single equation:

$$m = \frac{2.35\left(2 + 0.175Re_p^{0.75}\right)}{1 + 0.175Re_p^{0.75}} \tag{4}$$

Equations 3 and 4 can be used to show that m decreases as D, and therefore $w_{s,0}$, is increased. This also means that for every C-value the hindered settling effect, expressed as $w_{s,h}/w_{s,0}$ in Equation 1, increases with decreasing particle size. Hence, silt-sized particles (D = 0.004–0.063 mm) are more prone to hindered settling than sand-sized particles (D = 0.063–2 mm) in the transitional regime shown in Equation 3.

2.3 | Additional controls on hindered settling

The above hindered settling equations are approximations that do not account for modifications of the hindered settling effect by wall effects, particle shape, particle size distribution (sorting) and cohesive forces.

Wall effects describe reductions in fall velocity by friction at the walls of cylinders used to perform settling column and fluidisation experiments (Brea et al., 1976; Loeffler, 1953; Loeffler & Ruth, 1959). Richardson and Meikle (1961) proposed a modification of Equation 3 by including a parameter D/d, where D is the particle size and d is the diameter of the cylinder. Other modifications of hindered settling parameterisations were published by Neužil and Hrdina (1965), Rajagopalan and Laddha (1967), Ghosal and Mukherjea (1970), Garside and Al-Dibouni (1977) and Scott (1984), who included the wall effect in a thorough comparison of different hindered settling equations before proposing a modification of Equation 3 similar to that of Richardson and Meikle (1961). However, Di Felice (1995) concluded that the wall effect is poorly defined, questioning the D/d-type extensions of the Richardson and Zaki (1954a) equation. The limitations of the correction factor of Richardson and Meikle (1961) were also highlighted by Chong et al. (1979). For most practical purposes in sedimentology, however, the wall effect is considered negligible, because Ghosal and Mukherjea (1970) showed that the wall effect is important only for $D/d > 0.05$, even if it is considered that this threshold varies with Re_p (Fidleris & Whitmore, 1961). Hence, small cylinders with a diameter of at least 40 mm are sufficient to prevent reductions in settling velocity by wall friction for all sand and silt particle suspensions. Larger cylinders are needed for gravel-sized particles.

Particle shape has been demonstrated to have a significant effect on the hindered settling velocity. Richardson and Zaki (1954a), Fouda and Capes (1977), Chong et al. (1979), Chianese et al. (1992) and Baldock et al. (2004)

showed convincingly that the m-values in Equation 1 are lower for spherical particles than for non-spherical particles, because the particle density, and therefore the settling velocity, is reduced by the capture of stagnant fluid in the angularities of the non-spherical particles (Steinour, 1944b; Whitmore, 1956). Correction factors for particle shape were proposed by Steinour (1944b), Richardson and Zaki (1954a), Fouda and Capes (1977), Cleasby and Fan (1981) and Dharmarajah and Cleasby (1986), but these require laborious measurements of sphericity and angularity of individual particles. Di Felice (1995) found that the shape correction factor of Steinour (1944b) nearly always predicts an increase in particle volume by 20%–30%, which is equivalent to a 2.7%–3.1% increase in the diameter of spherical particles. This might apply especially to non-cohesive siliciclastic sediment grains, which usually approximate a spherical shape.

The effect of particle size distribution, or sorting, on the hindered settling effect is less clear than the effect of particle shape. Wilson (1953) showed that in low-density suspensions of poorly sorted populations of particles, the falling particles segregate because of differences in settling velocity, causing the hindered settling velocity to be less than for well-sorted populations with the same mean size. This is because the finer particles that segregate to the top of the suspension need longer to settle than the particles of mean size in the population. In contrast, particles do not segregate in high-density suspensions because smaller particles cannot easily pass through the gaps between larger particles, and the hindered settling velocity of poorly sorted and well-sorted particle populations were found to be similar (Wilson, 1953). However, the suspension concentration at which particle segregation changes into uniform settling of all particle sizes is unclear, and this threshold concentration is probably dependent on the particle size distribution itself.

Hoffman et al. (1960) showed that, in suspensions with segregating particle sizes, the total mass concentration of particles in a fluidised bed can be estimated from the sum of the mass concentrations of each particle size class. However, this might be more difficult to apply to continuous particle size distributions, which are typical of most applications, than for mixtures of discrete well-sorted particle populations. Wen and Yu (1966) defined an equivalent particle diameter for bimodal suspensions that can be used if the particle size ratio is less than 1.3, at which segregation does not occur. If this ratio is larger than 1.3, and segregation in two layers takes place, the particle concentration can be computed separately for each layer.

Correction factors for particle sorting in hindered settling equations are rare. Mirza and Richardson (1979) provided a modified hindered settling equation for sediment mixtures in the viscous regime, which allows for particle interactions, and Brauer and Kriegel (1966) proposed a theoretical model for hindered settling, also in the viscous regime, but only for bimodal size distributions. Based on physical theory, Maude and Whitmore (1958) proposed a simple extension of Equation 1 by replacing coefficient m with $4.65/a$, where $a = 1$ for $Re_p \leq 1$, $a = 2$ for $Re_p \geq 1000$ and $1 < a < 2$ for $1 < Re_p < 1000$ to allow for differences in particle shape and particle size distribution. However, Maude and Whitmore (1958) did not present sufficient evidence that a is independent of particle shape and sorting in the viscous and inertial regimes, and they did not support their theory with functional relationships between a and particle shape and sorting in the transitional regime.

Suspensions of cohesive particles have m-values that are significantly larger than those predicted by Equation 3, because cohesive forces can dramatically reduce the bulk settling rate (Johnson et al., 2016; Spearman & Manning, 2017; Wan & Wang, 1994). In other words, cohesive forces significantly magnify the hindered settling effect by providing supportive strength.

3 | METHODOLOGIES

3.1 | Metadata compilation

For the present metadata study, hindered settling data were extracted from 53 publications and 548 settling column and fluidisation experiments (Supplementary Table S1), which permitted re-validation of the m-values in the hindered settling equation of Richardson and Zaki (1954a) (Equation 1), and their relationship with particle Reynolds number (Equations 2 and 3). The settling behaviour of cohesive particles was excluded (Manning et al., 2010; Soulsby et al., 2013), because Equations 3 and 4 are not valid for particles that form flocculated or gelled suspensions. Several of the publications in the metadata study gave m-values and Re_p-values in tables or graphs. Other publications provided relationships between hindered settling velocity and suspended particle concentration, from which the m-value could be determined using Equation 1. Where needed, the single-particle settling velocity was calculated using Soulsby (1997), based on mean or median particle diameter, particle density and fluid viscosity. In papers in which the particle Reynolds number was not given, Re_p was calculated using single-particle settling velocity, mean or median particle diameter, particle density and fluid viscosity. If these properties were missing from the paper, they were extracted from standard tables for solids and liquids, assuming a temperature of 20°C, where applicable. The density of quartz grains and SiO_2-rich glass particles was assumed to be 2650 kg m^{-3} and the density and dynamic viscosity of water were assumed to be 1000 kg m^{-3} and 0.001 N s^{-1} m^{-2}, respectively, unless specified differently in the paper.

Before starting the metadata analysis, the literature data were assessed for potential quality issues and subdivided into high-quality and low-quality, because: (a) *m*-values need to be based on a wide range of particle concentrations for each Re_p-value (Di Felice, 1995; Riba & Couderc, 1977); here, data were required for $w_{s,h}/w_{s,0} > 0.4$; (b) at least five pairs of $w_{s,h}/w_{s,0}$ and *C* are needed to obtain accurate *m*-values; (c) the presence of cohesive forces may go undetected, resulting in excessively high *m*-values, and; (d) instead of a straight line, $\log_{10}(1 - C)$–$\log_{10}(w_{s,h}/w_{s,0})$ plots may take the shape of a curve, if the upward fluid flow in fluidisation experiments is non-uniform ('bubbling'), which is most common at small particle sizes and high particle concentrations (Di Felice, 1995), such as in one of the data sets of Wan and Wang (1994) (Supplementary Table S1).

3.2 | New hindered settling experiments

Five series of settling column experiments were conducted in the Hydrodynamics Laboratory of the School of Ocean Sciences (Bangor University) (Figure 1). These experiments used fresh water and well-sorted to very well-sorted spherical glass beads, produced by Guyson International Ltd. under the commercial name *Honite*, with the following mean sizes: 0.040 mm (coarse silt), 0.077 mm (very fine sand), 0.166 mm (fine sand), 0.382 mm (medium sand) and 0.552 mm (coarse sand). The diameter of the settling column was 73 mm, so D/d ranged from 5.5×10^{-4} for the coarse silt to 7.0×10^{-3} for the coarse sand. These values are well below $D/d = 0.05$, above which wall effects start to significantly reduce settling velocities (Ghosal & Mukherjea, 1970). In each series of experiments, $w_{s,h}$ was measured for at least eight different *C*-values between 5% and 55% by timing the falling interface between clear water and the settling suspension, that is, lutocline, in the column, after fully homogenising the starting suspension (Figure 1). Single-particle settling velocities were calculated with the Soulsby (1997) equation. The *m*-value for each particle size was then calculated from the slope gradient of a best-fit line between $\log_{10}(w_{s,h}/w_{s,0})$ and $\log_{10}(1 - C)$.

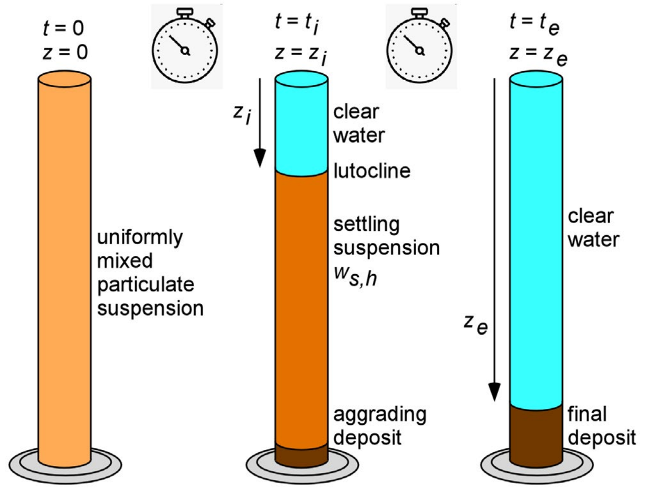

FIGURE 1 Schematic drawing of the set-up for the hindered settling experiments, where *t* is time, *z* is vertical distance and subscripts *i* and *e* denote 'intermediate' and 'end' respectively. The vertical position of the falling lutocline was recorded regularly until all particles had deposited. Because of the near-uniform grain size of the glass beads used in the experiments, the hindered settling velocity, $w_{s,h}$, was constant between $t = 0$ and $t = t_e$. The diameter of the settling column was 73 mm

4 | RESULTS

4.1 | New hindered settling experiments

The measured settling velocities for the different particle sizes are plotted against the suspended particle concentrations in Figure 2, which also shows the *m*-values calculated from the best-fit relationships between $w_{s,h}/w_{s,0}$ and $(1 - C)$. The *m*-values are all statistically significant, with $R^2 > 0.98$ and $p << 0.01$, and they range from 3.8501 for the coarse sand to 5.4184 for the coarse silt (Supplementary Table S1). Following the modification of Equation 3 for D/d of Richardson and Meikle (1961), the settling column width had no influence on the hindered settling velocity in the fine, medium and coarse sands, and the hindered settling velocity was reduced by 0.67% and 0.14% for the very fine sand and the coarse silt respectively. These errors are smaller than the accuracy with which the settling velocity could be measured in the experimental set-up, thus confirming the above inference, based on Ghosal and Mukherjea's (1970) criterion, that wall effects were negligible. Figure 3 shows that *m* decreased as Re_p was increased. This agrees with previous settling column and fluidisation experiments (Richardson & Zaki, 1954a).

4.2 | Metadata

The *m*-values and Re_p-values extracted from the hindered settling literature sources (Supplementary Table S1) are plotted in Figure 4. These data are subdivided into high-quality and low-quality data based on the four criteria mentioned in the Methodologies section. Figure 4 also shows the new experimental data. The low-quality data typically have higher *m*-values than most of the high-quality data, suggesting that narrow ranges of *C*-values,

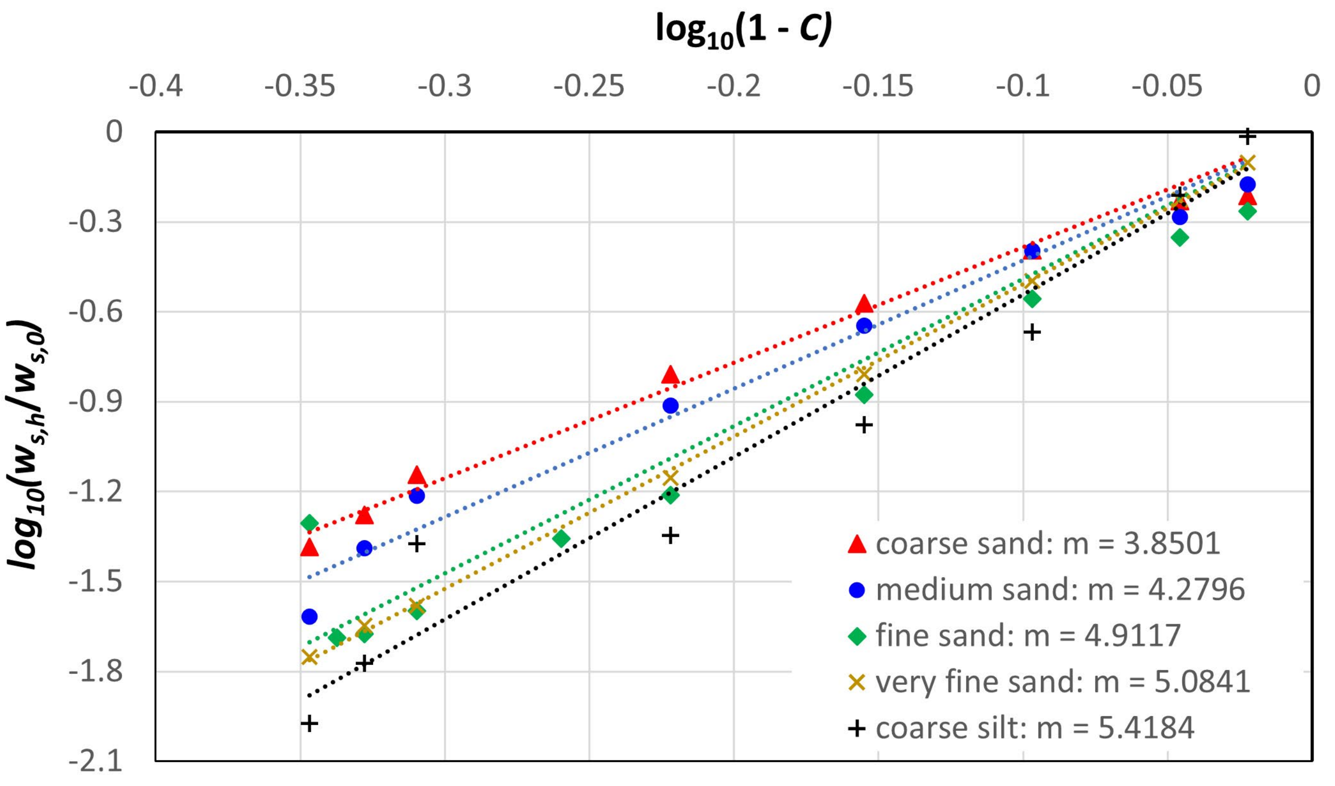

FIGURE 2 New experimental hindered settling data for five different particle sizes plotted as $\log_{10}(1-C)$ against $\log_{10}(w_{s,h}/w_{s,0})$, where the slopes of the best-fit lines represent the coefficient m of Equation 1 (Richardson & Zaki, 1954a)

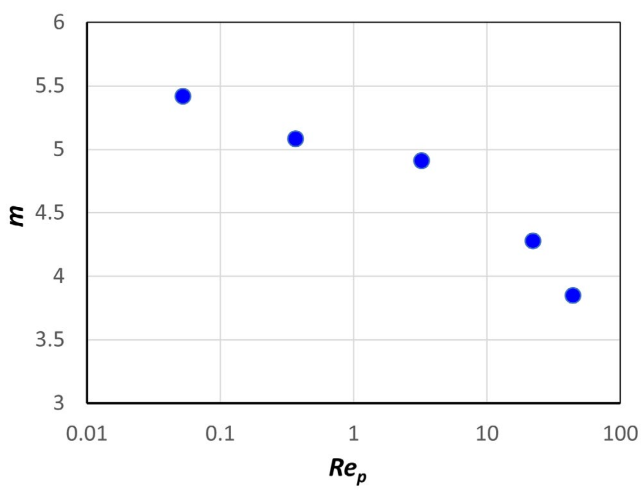

FIGURE 3 Particle Reynolds number, Re_p, against coefficient m of Equation 1 (Richardson & Zaki, 1954a) for the new experimental hindered settling data

mostly expressed as a lack of settling velocities at low particle concentrations, small data sets, 'bubbling' effects, and possibly also undetected cohesive forces, tend to over predict the hindered settling effect. This over prediction appears to be larger for smaller Re_p, decreasing from one to two orders of difference in $w_{s,h}/w_{s,0}$ in the viscous regime (here defined as $Re_p \leq 0.1$), via one order of difference in the transitional regime ($0.1 < Re_p < 500$), to less than one order of difference in the inertial regime ($Re_p \geq 500$). The new experimental data (green data points in Figure 4) follow the main trend of the literature data reasonably well.

The hindered settling data for spherical particles and natural sediment, for high-quality data sources only, are compared in Figure 5. This $m - Re_p$ graph thus focusses on sedimentological applications and a first-order appraisal of the effect of particle angularity, since most natural sediment is composed of near-spherical particles. Figure 5 reveals that natural sediment tends to have larger m-values than spherical particles in the transitional regime, but this difference decreases as Re_p is increased. However, natural sediment and spherical particles have similar m-values in the inertial regime, which corresponds to settling quartz granules and pebbles in fresh water at 20°C. Apparently, the strengthening of hindered settling because of capture of stagnant water in the angularities of rough spheres (Steinour, 1944b; Whitmore, 1956) is more effective for smaller particles with lower settling velocities than for larger particles with higher settling velocities. In other words, the hindered settling velocity of angular very fine sand is reduced more than that of angular very coarse sand in fresh water at 20°C.

The hindered settling data of quartz spheres and natural sediment in water are compared to the remainder of

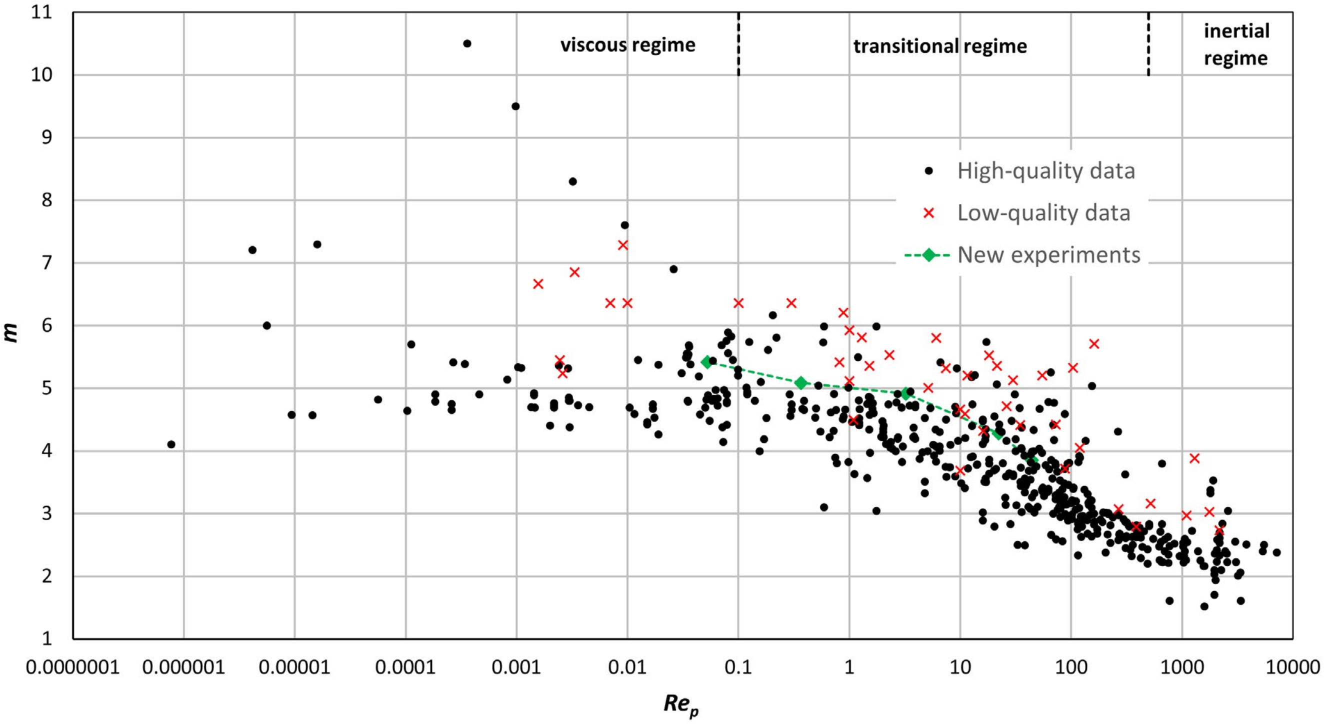

FIGURE 4 Particle Reynolds number, Re_p, against coefficient m of Equation 1 (Richardson & Zaki, 1954a) for all data collated, subdivided into high-quality and low-quality data sets

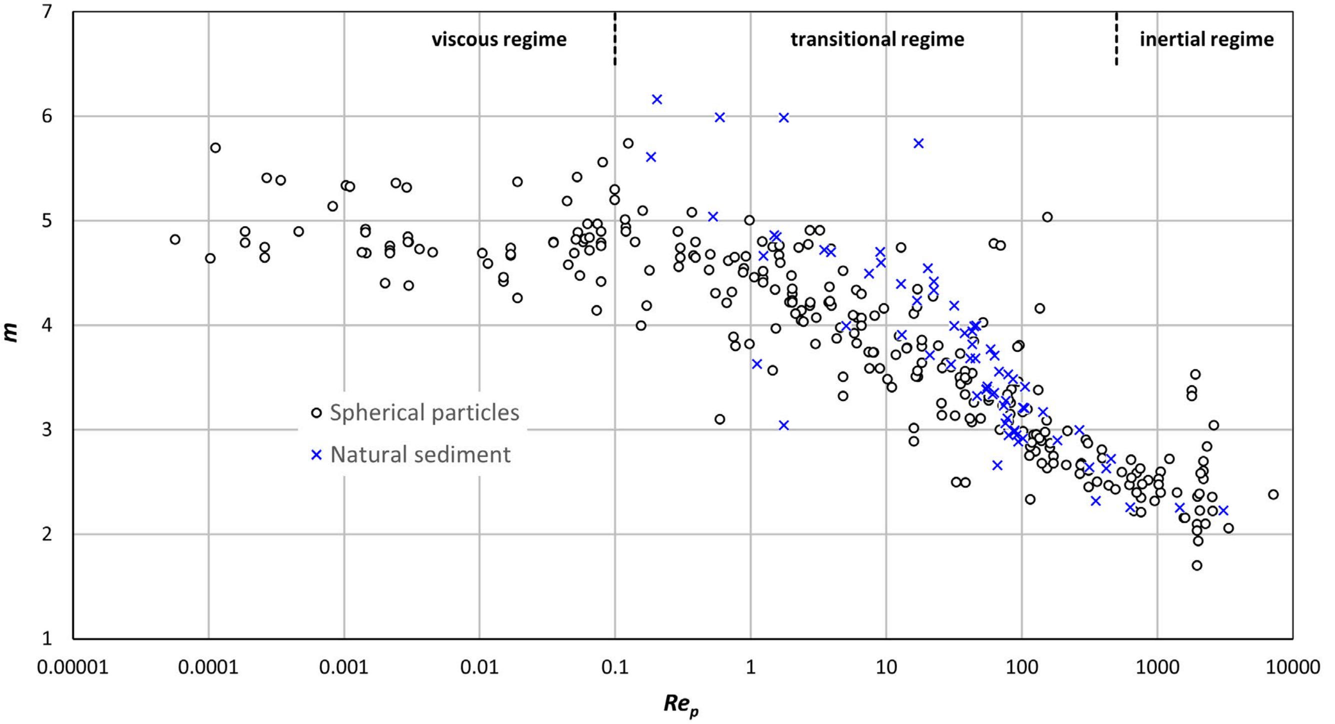

FIGURE 5 Particle Reynolds number, Re_p, against coefficient m of Equation 1 (Richardson & Zaki, 1954a) for spherical particles and natural sediment

the high-quality literature data in Figure 6, showing a lack of separation between these data sources. This confirms earlier inferences with smaller data sets (Richardson & Zaki, 1954a) that Re_p is a suitable parameter for quantifying hindered settling based on widely different fluids and solids, and that data from different disciplines can be used to develop a hindered settling parameter for use in sedimentology. Figure 6 therefore includes granulometric boundaries based on quartz grains settling in fresh water at 20°C, with the boundaries between the viscous and transitional regimes, $Re_p = 0.1$, and between the transitional and inertial regime, $Re_p = 500$, positioned in coarse silt and granule grades respectively. The spread in the m-values in Figure 6 is considerable, but acceptable for sedimentological applications, most probably caused by experimental error, wall effects, particle shape (sphericity and angularity), sorting and undetected cohesive forces.

5 | DISCUSSION

5.1 | Metadata-based hindered settling equation

The relationship between m and Re_p for the high-quality data presented in Figure 6 is similar to, but more accurate than, the relationship proposed by Richardson and Zaki (1954a) in Equation 3. The m-values in the viscous and inertial regime are constant, whereas m decreases, as Re_p is increased, in two steps in the transitional regime, but with updated fitting coefficients and different functions for the transitional regime (red dashed curve in Figure 6):

$$m = 5.037 \text{ for } Re_p \leq 0.1 \text{ (viscous regime)} \quad (5a)$$

$$m = 4.565 - 0.472 \log_{10}(Re\neg_p) \text{ for } 0.1 < Re_p \leq 10 \text{ (transitional regime)} \quad (5b)$$

$$m = 5.074 - 0.981 \log_{10}(Re\neg_p) \text{ for } 10 < Re_p < 500 \text{ (transitional regime)} \quad (5c)$$

$$m = 2.436 \text{ for } Re_p \geq 500 \text{ (inertial regime)} \quad (5d)$$

The four outliers at $Re_p \leq 0.026$ and $m \geq 6.9$ were discarded from the curve fitting procedure, because the rough methyl-methacrylate polymers used in these experiments behaved as soft rather than solid particles, causing an anomalously high hindered settling effect (Whitmore, 1956). The log-linear functions for the transitional regime

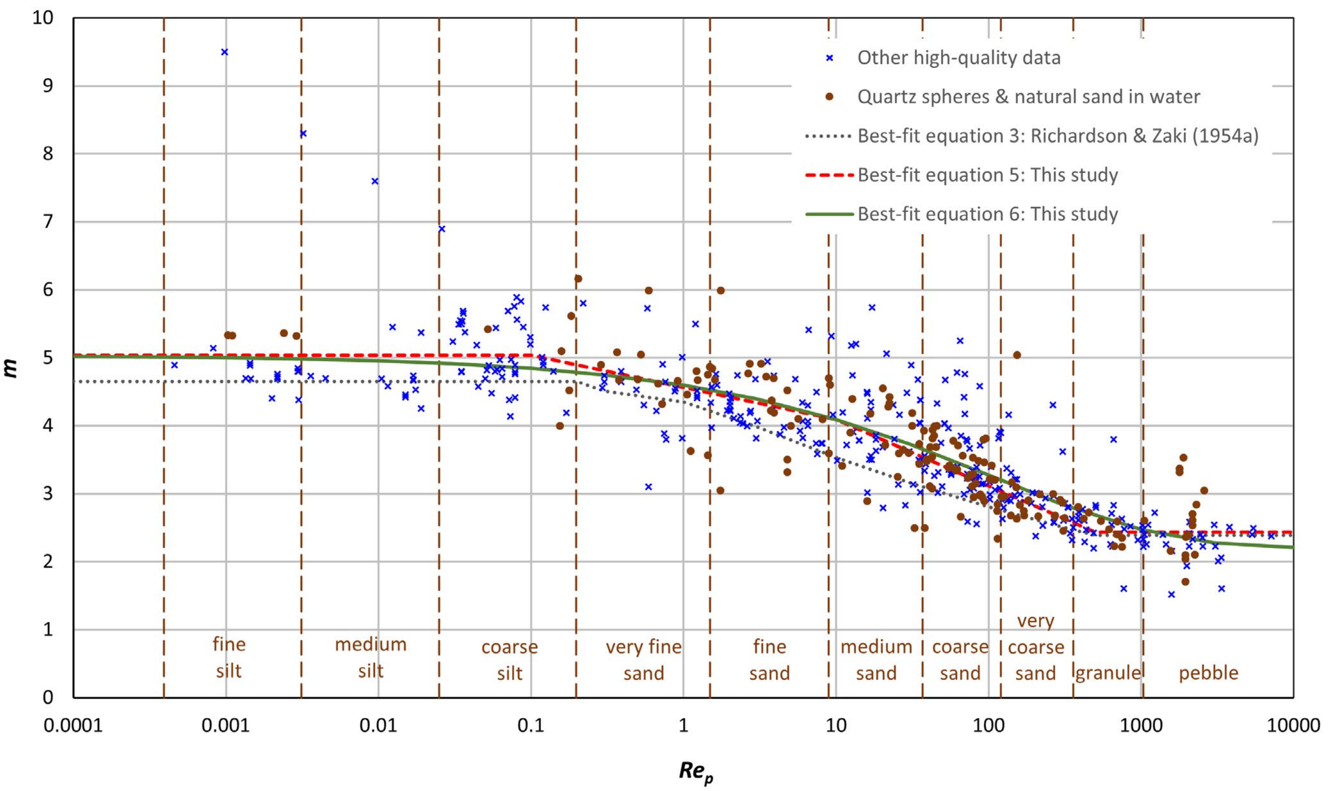

FIGURE 6 Particle Reynolds number, Re_p, against coefficient m of Equation 1 (Richardson & Zaki, 1954a) for quartz spheres and natural sediment in water, contrasted with other high-quality data. The abscissa is subdivided into grain-size classes based on the Wentworth scale, assuming quartz particles in 20°C fresh water. The red dashed and green continuous best-fit curves are based on Equations 5 and 6 respectively. The grey curve represents Equation 3 (Richardson & Zaki, 1954a); Except for pebbles, Equation 3 underestimates m-values and therefore also underestimates the hindered settling effect

(Equations 5b and 5c) are preferred over the power functions in Equation 3, because these appear as straight lines in Figure 6. For quartz particles in 20°C water, Equations 5a–d are valid approximately for silt, very fine and fine sand, medium to very coarse sand, and gravel respectively.

Equation 5 can be approximated by the following continuous best-fit equation (continuous green curve in Figure 6):

$$m = 5.037 - 2.839\left(1 - e^{-0.1687 Re_{\mathrm{p}}^{0.38}}\right) \tag{6}$$

Equation 6 performs well in comparison to Equation 5, but it predicts slightly lower m-values in the coarse silt range, slightly higher m-values for coarse sand to granules, and it does not predict a constant m-value at $Re_{\mathrm{p}} \geq 500$ (Figure 6).

5.2 | Importance of hindered settling in practical applications

Suspended particle concentration, C, is plotted against hindered settling effect, $w_{\mathrm{s,h}}/w_{\mathrm{s,0}}$, in Figure 7 for quartz particles settling in fresh water at 20°C. The particle diameters cover silt, sand and gravel, for each of which $w_{\mathrm{s,h}}/w_{\mathrm{s,0}}$ was calculated using Equations 1, 2 and 6. Figure 7 confirms earlier experimental and theoretical studies that the hindered settling effect increases as the particle size decreases (cf., Richardson & Zaki, 1954a, 1954b). For example, a 50% reduction in settling velocity is reached for 0.025 mm silt at $C = 13\%$ and for 4 mm pebbles at $C = 25\%$. Moreover, hindered settling starts to influence the settling behaviour of sediment particles at remarkably low concentrations. It can be deduced from Figure 7 that the particle settling velocity in flows that carry 5% silt is reduced by at least 22%, but even in coarse sand this reduction is 14%–17%. Such a C-value is low compared to that of many hyperconcentrated river flows and subaqueous sediment gravity flows, for example, debris flows, and marine and lacustrine turbidity currents (Talling, et al., 2012). This strong hindered settling effect at low particle concentrations is supported by McNown and Lin (1952), who found for 0.1 mm sand that 'for concentrations of a few tenths of a per cent by weight the actual settling velocity is 10% to 15% less than the single-particle settling velocity, in comparison with a reduction of about 30% for a concentration of 5%'. Oliver (1961), Bogárdi (1978), and Davis and Acrivos (1985) found similar hindered settling effects in low particle concentrations despite the fact that hindered settling equations tend to slightly under predict settling velocities at low particle concentrations (Di Felice, 1995; Riba & Couderc, 1977).

Settling velocities in numerical models of the kinematics of sediment-laden flows should therefore account for the hindered settling effect more often to avert under predictions of deposit runout distances. Conversely, the results of this study imply that the strong hindered settling effect, even at low suspended sediment concentrations and particularly for fine, non-cohesive sediment, helps to explain the high efficiency of bottom-hugging sediment gravity flows in the deep-marine environment, and the long distance of transport of their sediment load (Talling et al., 2007). The strong hindered settling effect thus helps to maintain the main driving force of sediment gravity flows, which is the density difference between the flow and the ambient water. At the experimental scale, this strong hindered settling may have contributed to the high head velocity of sediment gravity flows that carried medium silt-sized silica flour at volumetric concentrations of up to 49% on a horizontal slope (Baker et al., 2017; their figure 10A). Moreover, the strong hindered settling effect needs to be included in studies defining depositional and erosional regimes for sediment gravity flows. This includes the study by Halsey et al. (2017), who used settling velocity to define weak and moderate–strong erosional regimes as well as high-Rouse number and turbulence-suppression induced depositional regimes for natural sediment gravity flows. It is expected that incorporating the hindered settling effect, that is, Equations 5 and 6, would change the boundaries between these regimes, and thus changes predicted patterns of erosion and deposition.

5.3 | Future research directions and new measurement methods

Improved understanding of hindered settling dynamics in natural and synthetic particle suspensions can benefit a wide range of applications, including the role of hindered settling for dense suspensions in the geological past. This paper demonstrates significant hindered settling effects on particle fall velocities in relatively low concentration suspensions for silt-grade particles. Below, the focus is on fertile areas of sedimentological research that require further investigations to consider the range of the settling velocities of particles in dense and dilute suspensions.

A better understanding of particle hydrodynamics during hindered settling, and therefore improved predictions of transport and depositional patterns of particles, is essential to address several sedimentological 'grand challenges' (Hodgson et al., 2018). These include predictions of where concentrations of anthropogenic pollutants, such as terrestrial organic carbon in marine environments (Baudin et al., 2017) and microplastics (Kane et al., 2020), are highest, as these materials can be transported via

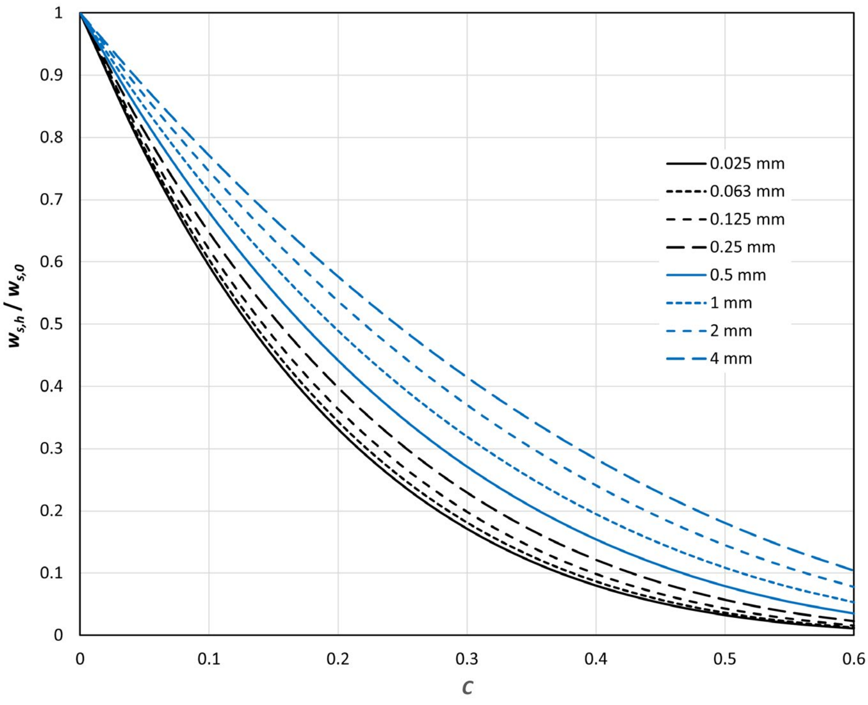

FIGURE 7 Suspended particle concentration, C, against hindered settling effect, $w_{s,h}/w_{s,0}$, for quartz particles settling in fresh water at 20°C. The particle diameters cover silt, sand and gravel, for which $w_{s,h}/w_{s,0}$ was calculated using Equations 1, 2 and 6

particulate density currents (Zhong & Peng, 2021), bottom currents (Kane et al., 2020), and via settling out from suspension. Long-term burial of particulate terrestrial organic carbon in marine sediment removes CO_2 from the atmosphere, helping to regulate the global climate. The burial efficiency of terrestrial organic carbon in marine sediment depends on the exposure time to oxygen, which ties back to suspension settling rates. In terms of anthropogenic pollutants, sea surface accumulations of plastics account for *ca* 1% of the estimated global marine plastic budget (Koelmans et al., 2017; Thompson et al., 2004). Much of this plastic occurs as micro-scale (0.1 μm–5 mm) fragments, pellets and fibres. Yet, their distribution in the marine water column and depositional environments by, in particular, dense sediment gravity flows, in which hindered settling plays a pivotal role, is poorly understood.

Physical-chemical-biological particle interactions is another area that will benefit from improved understanding of hindered settling processes. In particular, the role of animal-sediment interactions, for example, via bioturbation, has been shown to coat clastic particles in clay rims that range from patchy to fully coated (Dowey et al., 2017). The partial coating of grains with clay forms cohesive sediment mixtures, which when remobilised can generate highly dynamic changes in grain size and shape distributions during transport, and decrease bulk settling rates (Johnson et al., 2016). Furthermore, the recognition that sedimentary processes are strongly influenced by extracellular polymeric substances (EPS), and other cohesive fine-grained material (Lai et al., 2018; Lichtman et al., 2018; Malarkey et al., 2015; Parsons et al., 2016; Tolhurst et al., 2002), complicates studies that aim to constrain deposits from polydisperse flows of mixed particle size, shape and density, including mixtures of cohesive and non-cohesive particles. Investigations of physical-chemical-biological particle interactions that include hindered settling effects in such flows will refine bedform-phase diagrams that at present assume narrow, monodisperse, grain-size distributions, leading to reanalysis of many sedimentary structures and process interpretations (Baas et al., 2016).

New technologies permit investigations into the role of particle size and shape distributions, the behaviour of composite particles with different densities, and the influence of changing density and viscosity of ambient fluids. These can test the new empirical equation for hindered settling of non-cohesive particles proposed here, and natural systems that contain particles with complex shapes, mixed grain populations and cohesive forces. An available measurement technique, used in combination with the settling column method (Wilson, 1952, 1953), is particle imaging velocimetry (Di Cristo, 2011). Particle imaging velocimetry allows high-precision measurements of particle trajectories and accelerations, and the resultant pressure field and drag effects within a measurement volume. It is possible to make high-resolution three-dimensional measurements of falling particles during settling, including hindered settling, of microplastics, and other low-density particles with complex morphologies, such as clay flocs and organic carbon particles, in controlled physical experiments. Such experiments are needed to inform numerical models that aim to predict long-term and large-scale dispersal and concentration of particles.

6 | CONCLUSIONS

The compilation of hindered settling data from multiple disciplines for this paper has returned an improved empirical equation for hindered settling of non-cohesive particles compared to the widely used equation of Richardson and Zaki (1954a). The new equation confirms that the hindered settling velocity increases with decreasing particle size. For example, a 50% reduction in settling velocity is reached for 0.025 mm silt and 4 mm pebbles at particle concentrations of 13% and 25% respectively. Hindered settling also starts to influence the settling behaviour of sediment particles at low concentrations, for example, flows that carry 5% silt experience a reduction in settling velocity by at least 22%. These results imply that the hindered settling effect needs to be included routinely in research and applications that comprise settling velocities.

ACKNOWLEDGEMENTS

The authors are grateful to Equinor Norway for funding part of this research through a grant to Baas and Baker, which also partially contributed to Buffon's visit to the Hydrodynamics Laboratory at Bangor University from the Federal University of Rio Grande do Sul. The authors also wish to thank the TNA access to EPOS multi-scale laboratory facilities programme at Utrecht University, which funded the hindered settling metadata analysis, and related experimental work intended for a separate paper. William Morgan kindly assisted in the hindered settling experiments. An earlier version of this paper benefitted from the detailed comments by an anonymous reviewer and the Associate Editor.

DATA AVAILABILITY STATEMENT

The data that support the findings of this study are available from the corresponding author upon reasonable request.

ORCID

Jaco H. Baas https://orcid.org/0000-0003-1737-5688
David Hodgson https://orcid.org/0000-0003-3711-635X
Yvonne T. Spychala https://orcid.org/0000-0002-3896-9234

REFERENCES

Baas, J.H., Best, J.L. & Peakall, J. (2016) Predicting bedforms and primary current stratification in cohesive mixtures of mud and sand. *Journal of the Geological Society*, *173*, 12–45.

Baker, M.L., Baas, J.H., Malarkey, J., Jacinto, R.S., Craig, M.J., Kane, I.A. & Barker, S. (2017) The effect of clay type on the properties of cohesive sediment gravity flows and their deposits. *Journal of Sedimentary Research*, *87*, 1176–1195.

Baldock, T.E., Tomkins, M.R., Nielsen, P. & Hughes, M.G. (2004) Settling velocity of sediments at high concentrations. *Coastal Engineering*, *51*, 91–100.

Barnea, E. & Mizrahi, J. (1973) A generalised approach to the fluid dynamics of particulate systems: part 1. General correlation for fluidization and sedimentation in solid multiparticle systems. *The Chemical Engineering Journal*, *5*, 171–189.

Baudin, F., Martinez, P., Dennielou, B., Charlier, K., Marsset, T., Droz, L. & Rabouille, C. (2017) Organic carbon accumulation in modern sediments of the Angola basin influenced by the Congo deep-sea fan. *Deep Sea Research Part II: Topical Studies in Oceanography*, *142*, 64–74.

Bell, D., Soutter, E.L., Cumberpatch, Z.A., Ferguson, R.A., Spychala, Y.T., Kane, I.A. & Eggenhuisen, J.T. (2021) Flow-process controls on grain type distribution in an experimental turbidity current deposit: implications for detrital signal preservation and microplastic distribution in submarine fans. *The Depositional Record*, *7*(3), 392–415. https://doi.org/10.1002/dep2.153.

Beňa, J., Ilavský, J., Kossaczský, E. & Neužil, L. (1963) Changes of the flow character in a fluidized bed. *Collection of Czechoslovak Chemical Communications*, *28*, 293–309.

Bogárdi, J. (1978) *Sediment transport in alluvial streams*. Budapest: Akademiai Kiado, p. 826.

Brauer, H. & Kriegel, E. (1966) Kornbewegung bei der Sedimentation. *Chemie Ingenieur Technik*, *38*, 321–330.

Brea, F.M., Edwards, M.F. & Wilkinson, W.L. (1976) The flow of non-Newtonian slurries through fixed and fluidised beds. *Chemical Engineering Science*, *31*, 329–336.

Brinkman, H.C. (1949) A calculation of the viscous force exerted by a flowing fluid on a dense swarm of particles. *Applied Scientific Research*, *A1*, 27–34.

Camenen, B. (2007) Simple and general formula for the settling velocity of particles. *Journal of Hydraulic Engineering*, *133*, 229–233.

Carey, V.P. (1987) Dependence of settling velocity on particle concentration in a fluidised bed of spherical particles. *International Journal of Multiphase Flow*, *13*, 429–431.

Cheng, N.-S. (1997) Effect of concentration on settling velocity of sediment particles. *Journal of Hydraulic Engineering*, *123*, 728–731.

Chianese, A., Frances, C., Di Berardino, F. & Bruno, L. (1992) On the behaviour of a liquid fluidized bed of monosized sodium perborate crystals. *The Chemical Engineering Journal*, *50*, 87–94.

Chong, Y.S., Ratkowsky, D.A. & Epstein, N. (1979) Effect of particle shape on hindered settling in creeping flow. *Powder Technology*, *23*, 55–66.

Cleasby, J.L. & Fan, K. (1981) Predicting fluidization and expansion of filter media. *Journal of Environmental Engineering*, *107*, 455–471.

Davis, R.H. & Acrivos, A. (1985) Sedimentation of noncolloidal particles at low Reynolds numbers. *Annual Review of Fluid Mechanics*, *17*, 91–118.

Dharmarajah, A.H. & Cleasby, J.L. (1986) Predicting the expansion behavior of filter media. *Journal of the American Water Works Association*, *78*, 66–76.

Di Cristo, C. (2011) Particle imaging velocimetry and its applications in hydraulics: a state-of-the-art review. In: Rowinski, P. (Ed.) *Experimental methods in hydraulic research*, Geoplanet: Earth and Planetary Sciences book series, *1*, 49–66.

Di Felice, R. (1995) Hydrodynamics of liquid fluidisation. *Chemical Engineering Science*, *50*, 1213–1245.

Di Felice, R. (1996) The particle-in-a-tube analogy for a multiparticle suspension. *International Journal of Multiphase Flow*, *22*, 515–525.

Dietrich, W.E. (1982) Settling velocity of natural particles. *Water Resources Research*, *18*, 1615–1626.

Dowey, P.J., Worden, R.H., Utley, J. & Hodgson, D.M. (2017) Sedimentary controls on modern sand grain coat formation. *Sedimentary Geology*, *353*, 46–63.

Ferguson, R.I. & Church, M. (2004) A simple universal equation for grain settling velocity. *Journal of Sedimentary Research*, *74*, 933–937.

Fidleris, V. & Whitmore, R.L. (1961) Experimental determination of the wall effect for spheres falling axially in cylindrical vessels. *British Journal of Applied Physics*, *12*, 490–494.

Foscolo, P.U., Gibilaro, L.G. & Waldram, S.P. (1983) A unified model for particulate expansion of fluidised beds and flow in fixed porous media. *Chemical Engineering Science*, *38*, 1251–1260.

Fouda, A.E. & Capes, C.E. (1977) Hydrodynamic particle volume and fluidized bed expansion. *The Canadian Journal of Chemical Engineering*, *55*, 386–391.

Garside, J. & Al-Dibouni, M.R. (1977) Velocity–voidage relationships for fluidization and sedimentation in solid–liquid systems. *Industrial & Engineering Chemistry Process Design & Development*, *16*, 206–214.

Ghosal, S.K. & Mukherjea, R.N. (1970) Schlupfgeschwindigkeit von Feststoffteilchen in absatzweise betriebenen Fest/flüssig-Wirbelschichten. *Chemie Ingenieur Technik*, *42*, 81–85.

Godard, K. & Richardson, J.F. (1969) Correlation of data for minimum fluidising velocity and bed expansion particulately fluidised systems. *Chemical Engineering Science*, *24*, 363–367.

Halsey, T.C., Kumar, A. & Perillo, M.M. (2017) Sedimentological regimes for turbidity currents: depth-averaged theory. *Journal of Geophysical Research Oceans*, *122*, 5260–5285.

Happel, J. (1958) Viscous flow in multiparticle systems: Slow motion of fluids relative to beds of spherical particles. *AIChE Journal*, *4*, 197–201.

Happel, J. & Epstein, N. (1954) Cubical assemblages of uniform spheres. *Industrial & Engineering Chemistry*, *46*, 1187–1194.

Hodgson, D.M., Bernhardt, A., Clare, M.A., Da Silva, A.C., Fosdick, J.C., Mauz, B., Midtkandal, I., Owen, A. & Romans, B.W. (2018) Grand challenges (and great opportunities) in sedimentology, stratigraphy, and diagenesis research. *Frontiers in Earth Science*, *6*, 173.

Hoffman, R.F., Lapidus, L. & Elgin, J.C. (1960) The mechanics of vertical moving fluidized systems: IV. Application to batch-fluidized systems with mixed particle sizes. *AIChE Journal*, *6*, 321–324.

Johnson, M., Peakall, J., Fairweather, M., Biggs, S., Harbottle, D. & Hunter, T.N. (2016) Characterization of multiple hindered settling regimes in aggregated mineral suspensions. *Industrial & Engineering Chemistry Research*, *55*, 9983–9993.

Jottrand, R. (1952) An experimental study of the mechanism of fluidization. *Journal of Applied Chemistry*¸, *2*, 517–526.

Kane, I.A., Clare, M.A., Miramontes, E., Wogelius, R., Rothwell, J.J., Garreau, P. & Pohl, F. (2020) Seafloor microplastic hotspots controlled by deep-sea circulation. *Science*, *368*, 1140–1145.

Kermack, W.O., M'Kendrick, A.G. & Ponder, E. (1930) The stability of suspensions: III. The velocities of sedimentation and of cataphoresis of suspensions in a viscous fluid. *Proceedings of the Royal Society of Edinburgh*, *49*, 170–197.

Khan, A.R. & Richardson, J.F. (1989) Fluid–particle interactions and flow characteristics of fluidized beds and settling suspensions of spherical particles. *Chemical Engineering Communications*, *78*, 111–130.

Koelmans, A.A., Kooi, M., Law, K.L. & Van Sebille, E. (2017) All is not lost: deriving a top-down mass budget of plastic at sea. *Environmental Research Letters*, *12*, 114028.

Komar, P.D. & Reimers, C.E. (1978) Grain shape effects on settling rates. *Journal of Geology*, *86*, 193–209.

Kynch, G.J. (1959) Sedimentation and affective viscosity. *Nature*, *184*, 1311.

Lai, H., Fang, H., Huang, L., He, G. & Reible, D. (2018) A review on sediment bioflocculation: dynamics, influencing factors and modelling. *Science of the Total Environment*, *642*, 1184–1200.

Letan, R. (1974) On vertical dispersed two-face flow. *Chemical Engineering Science*, *29*, 624–626.

Lewis, E.W. & Bowerman, E.W. (1952) Fluidization of solid particles in liquid. *Chemical Engineering Progress*, *48*, 603–610.

Lewis, W.K., Gilliland, E.R. & Bauer, W.C. (1949) Characteristics of fluidized particles. *Industrial & Engineering Chemistry*, *41*, 1104–1117.

Lichtman, I.D., Baas, J.H., Amoudry, L.O., Thorne, P.D., Malarkey, J., Hope, J.A., Peakall, J., Paterson, D.M., Bass, S.J., Cooke, R.D., Manning, A.J., Davies, A.G., Parsons, D.R. & Ye, L. (2018) Bedform migration in a mixed sand–mud intertidal environment and implications for bed material transport predictions. *Geomorphology*, *315*, 17–32.

Lockett, M.J. & Al-Habbooby, H.M. (1974) Relative particle velocities in two-species settling. *Powder Technology*, *10*, 67–71.

Loeffler, A.L. Jr (1953) *Mechanism of hindered settling and fluidisation*. Ph.D. Thesis, USA, Iowa State University, p. 83.

Loeffler, A.L. Jr & Ruth, B.F. (1959) Particulate fluidization and sedimentation of spheres. *AIChE Journal*, *5*, 310–314.

Malarkey, J., Baas, J.H., Hope, J.A., Aspden, R.J., Parsons, D.R., Peakall, J., Paterson, D.M., Schindler, R.J., Ye, L., Lichtman, I.D., Bass, S.J., Davies, A.G., Manning, A.J. & Thorne, P.D. (2015) The pervasive role of biological cohesion in bedform development. *Nature Communications*, *6*, 6257.

Manning, A.J., Baugh, J.V., Spearman, J. & Whitehouse, R.J.S. (2010) Flocculation settling characteristics of mud:sand mixtures. *Ocean Dynamics*, *60*, 237–253.

Maude, A.D. & Whitmore, R.L. (1958) A generalized theory of sedimentation. *British Journal of Applied Physics*, *9*, 477–482.

McNown, J.S. & Lin, P.-N. (1952) *Sediment concentration and fall velocity*. Reprints in Engineering. Issue 109, State University of Iowa, p. 11.

Mirza, S. & Richardson, J.F. (1979) Sedimentation of suspensions of particles of two or more sizes. *Chemical Engineering Science*, *34*, 447–454.

Neužil, L. & Hrdina, M. (1965) Effect of walls on the expansion of a fluidized bed. *Collection of Czechoslovak Chemical Communications*, *30*, 752–768.

Oliver, D.R. (1961) The sedimentation of suspensions of closely-sized spherical particles. *Chemical Engineering Science*, *15*, 230–242.

Pal, D. & Ghoshal, K. (2013) Hindered settling with an apparent particle diameter concept. *Advances in Water Resources*, *60*, 178–187.

Parsons, D.R., Schindler, R.J., Hope, J.A., Malarkey, J., Baas, J.H., Peakall, J., Manning, A.J., Ye, L., Simmons, S., Paterson, D.M., Aspden, R.J., Bass, S.J., Davies, A.G., Lichtman, I.D. & Thorne, P.D. (2016) The role of bio-physical cohesion on subaqueous bedform size. *Geophysical Research Letters*, *43*, 1566–1573.

Pyles, D.R., Straub, K.M. & Stammer, J.G. (2013) Spatial variations on the composition of turbidites due to hydrodynamic fractionation. *Geophysical Research Letters*, *40*, 3919–3923.

Rajagopalan, R. & Laddha, G.S. (1967) Liquid flow through fixed and fluidised beds. *Transactions of the Indian Institute of Chemical Engineering IX/3*, 83–87.

Ramamurthy, K. & Subbaraju, K. (1973) Bed expansion characteristics of annular liquid-fluidized beds. *Industrial & Engineering Chemistry Process Design & Development*, *12*, 184–189.

Riba, J.P. & Couderc, J.P. (1977) Expansion de couches fluidisées par des liquids. *The Canadian Journal of Chemical Engineering*, *55*, 118–121.

Richardson, J.F. & Meikle, R.A. (1961) Sedimentation and fluidisation: part III. The sedimentation of uniform fine particles and of two-component mixtures of solids. *Transactions of the Institute of Chemical Engineering*, *39*, 348–356.

Richardson, J.F. & Zaki, W.N. (1954a) Sedimentation and fluidisation, part I. *Transactions of the Institute of Chemical Engineering*, *32*, 35–53.

Richardson, J.F. & Zaki, W.N. (1954b) The sedimentation of a suspension of uniform spheres under conditions of the viscous flow. *Chemical Engineering Science*, *3*, 65–73.

Robinson, C.S. (1926) Some factors influencing sedimentation. *Industrial and Engineering Chemistry*, *18*, 869–871.

Rowe, P.N. (1987) A convenient empirical equation for estimation of the Richardson-Zaki exponent. *Chemical Engineering Science*, *42*, 2795–2796.

Scott, K.J. (1984) Hindered settling of a suspension of spheres: critical evaluation of equations relating settling rate to mean particle diameter and suspension concentration. *Council for Scientific and Industrial Research, Chemical Engineering Research Group, Report*, *497*, 101.

Scott, K.J. & Mandersloot, W.G.B. (1979) The mean particle size in hindered settling of multisized particles. *Powder Technology*, *24*, 99–101.

Shannon, P.T., Stroupe, E. & Tory, E.M. (1963) Batch and continuous thickening: basic theory, solids flux for rigid spheres. *I&EC Fundamentals*, *2*, 203–211.

Soulsby, R. (1997) *Dynamics of marine sands: a manual for practical applications*. London: Thomas Telford, p. 272.

Soulsby, R.L., Manning, A.J., Spearman, J. & Whitehouse, R.J.S. (2013) Settling velocity and mass settling flux of flocculated estuarine sediments. *Marine Geology*, *339*, 1–12.

Spearman, J. & Manning, A.J. (2017) On the hindered settling of sand-mud suspensions. *Ocean Dynamics*, *67*, 465–483.

Spychala, Y.T., Eggenhuisen, J., Tilston, M. & Pohl, F. (2020) The influence of basin settings and flow properties on the dimensions of submarine lobe elements. *Sedimentology*, *67*, 3471–3491.

Steinour, H.H. (1944a) Rate of sedimentation: nonflocculated suspensions of uniform spheres. *Industrial & Engineering Chemistry*, *36*, 618–624.

Steinour, H.H. (1944b) Rate of sedimentation: suspensions of uniform-size angular particles. *Industrial & Engineering Chemistry*, *36*, 840–847.

Stokes, G.G. (1851) On the effect of internal friction of fluids on the motion of pendulums. *Transactions of the Cambridge Philosophical Society*, *9*, part II, 8–106.

Talling, P.J., Masson, D.G., Sumner, E.J. & Malgesini, G. (2012) Subaqueous sediment density flows: depositional processes and deposit types. *Sedimentology*, *59*, 1937–2003.

Talling, P.J., Wynn, R.B., Masson, D.G., Frenz, M., Cronin, B.T., Schiebel, R., Akhmetzhanov, A.M., Dallmeier-Tiessen, S., Benetti, S., Weaver, P.P.E., Georgiopoulou, A., Zühlsdorff, C. & Amy, L.A. (2007) Onset of submarine debris flow deposition far from original giant landslide. *Nature*, *450*, 541–544.

Te Slaa, S., van Maren, D.S., He, Q. & Winterwerp, J.C. (2015) Hindered settling of silt. *Journal of Hydraulic Engineering*, https://doi.org/10.1061/(ASCE)HY.1943-7900.0001038.

Thompson, R.C., Olsen, Y., Mitchell, R.P., Davis, A., Rowland, S.J., John, A.W., McGonigle, D. & Russell, A.E. (2004) Lost at sea: where is all the plastic? *Science*, *304*, 838.

Tolhurst, T.J., Gust, G. & Paterson, D.M. (2002) The influence on an extra-cellular polymeric substance (EPS) on cohesive sediment stability. In: Winterwerp, J.C. & Kranenburg, C. (Eds.) *Fine sediment dynamics in the marine environment*, Proceedings in Marine Science, *5*, 409–425.

van Rijn, L.C. (1993) *Principles of sediment transport in rivers, estuaries and coastal seas*. Amsterdam: Aqua Publications, p. 700.

Wan, Z. & Wang, Z. (1994) *Hyperconcentrated flow (IAHR monograph)*. Rotterdam, Netherlands: Balkema, p. 230.

Watanabe, H. (1978) Voidage function in particulate fluid systems. *Powder Technology*, *19*, 217–225.

Wen, C.Y. & Fan, L.S. (1974) Some remarks on the correlation of bed expansion in liquid–solid fluidized beds. *Industrial & Engineering Chemistry Process Design & Development*, *13*, 194–197.

Wen, C.Y. & Yu, Y.H. (1966) Mechanics of fluidization. *Chemical Engineering Progress Symposium Series*, *62*, 100–111.

Whitmore, R.L. (1956) The relationship of the viscosity to the settling rate of slurries. *Journal of the Institute of Fuel*, *30*, 238–242.

Wilhelm, R.H. & Kwauk, M. (1948) Fluidization of solid particles. *Chemical Engineering Progress*, *44*, 201–218.

Wilson, B.W. (1952) The sedimentation of dilute suspensions of microscopic spheres in water. *Australian Journal of Applied Science*, *3*, 252–256.

Wilson, B.W. (1953) The sedimentation of dense suspensions of microscopic spheres. *Australian Journal of Applied Science*, *4*, 274–299.

Wu, W. & Wang, S.S.Y. (2006) Formulas for sediment porosity and settling velocity. *Journal of Hydraulic Engineering*, *132*, 858–862.

Zhong, G. & Peng, X. (2021) Transport and accumulation of plastic litter in submarine canyons—the role of gravity flows. *Geology*, *49*, 581–586.

Zuber, N. (1964) On the dispersed two-phase flow in the laminar flow regime. *Chemical Engineering Science*, *19*, 897–917.

SUPPORTING INFORMATION

Additional supporting information may be found in the online version of the article at the publisher's website.

How to cite this article: Baas, J.H., Baker, M.L., Buffon, P., Strachan, L.J., Bostock, H.C., Hodgson, D., Eggenhuisen, J.T. & Spychala, Y.T. (2022) Blood, lead and spheres: A hindered settling equation for sedimentologists based on metadata analysis. *The Depositional Record*, 00, 1–13. https://doi.org/10.1002/dep2.176